

# 1 **The Potamochemical symphony: new progress in the high-** 2 **frequency acquisition of stream chemical data**

3 Paul Floury<sup>1,2\*</sup>, Jérôme Gaillardet<sup>1</sup>, Eric Gayer<sup>1</sup>, Julien Bouchez<sup>1</sup>, Gaëlle Tallec<sup>2</sup>,  
4 Patrick Ansart<sup>2</sup>, Frédéric Koch<sup>3</sup>, Caroline Gorge<sup>1</sup>, Arnaud Blanchouin<sup>2</sup>, and Jean-Louis  
5 Roubaty<sup>1</sup>

6 <sup>1</sup> Institut de Physique du Globe de Paris (IPGP), CNRS and Université Sorbonne Paris-Cité, 1 rue Jussieu,  
7 75238 Paris, France

8 <sup>2</sup> UR HBAN, Institut national de recherche en sciences et technologies pour l'environnement et  
9 l'agriculture, Antony (IRSTEA), France

10 <sup>3</sup> Endress+Hauser SAS, Huningue, France

11 Corresponding author. E-mail: [floury@ipgp.fr](mailto:floury@ipgp.fr) and [gaillardet@ipgp.fr](mailto:gaillardet@ipgp.fr)

12

13 **Abstract.** Our understanding of hydrological and chemical processes at the catchment  
14 scale is limited by our capacity to record the full breadth of the information carried by  
15 river chemistry, both in terms of sampling frequency and precision. Here, we present a  
16 proof-of-concept study of a “lab in the field” called the “River Lab” (RL), based on the  
17 idea of permanently installing a suite of laboratory instruments in the field next to a  
18 river. **Housed in a small shed,** this set of instruments performs analyses at a frequency  
19 of one every 40 minutes for major dissolved species ( $\text{Na}^+$ ,  $\text{K}^+$ ,  $\text{Mg}^{2+}$ ,  $\text{Ca}^{2+}$ ,  $\text{Cl}^-$ ,  $\text{SO}_4^{2-}$ ,  
20  $\text{NO}_3^-$ ) through continuous sampling and filtration of the river water using automated ion  
21 chromatographs. The RL was deployed in the Orgeval Critical Zone Observatory,  
22 France for over a year of continuous analyses. Results show that the RL is able to  
23 capture long-term fine chemical variations with no drift and a precision significantly  
24 better than conventionally achieved in the laboratory (up to  $\pm 0.5\%$  for all major  
25 species for over a day and up to  $1.7\%$  over two months). The RL is able to capture the  
26 abrupt changes in dissolved species concentrations during a typical 6-day rain event, as

27 well as daily oscillations during a hydrological low-flow period of summer drought.  
28 Using the measured signals as a benchmark, we numerically assess the effects of a  
29 lower sampling frequency (typical of conventional field sampling campaigns) and of a  
30 lower precision (typically reached in the laboratory) on the hydrochemical signal. The  
31 high-resolution, high-precision measurements made possible by the RL open new  
32 perspectives for understanding critical zone hydro-bio-geochemical cycles. Finally, the  
33 RL also offers a solution for management agencies to monitor water quality in quasi  
34 real-time.

35

## 36 **1 Introduction**

37 Rivers are messengers from the Critical Zone. The chemical composition of rivers  
38 offers a window into the multiple processes that operate among water, organic matter,  
39 primary and secondary minerals and living organisms at the Earth's surface. (Calmels et  
40 al. 2011; Feng et al., 2004; Kirchner et al., 2000; Kirchner et al., 2001; Neal et al., 2012;  
41 Neal et al. 2013). Understanding the parameters that control the composition of river  
42 water is not only a scientific challenge, but also one of the major challenges for  
43 humanity to access and preserve drinkable water (Bain et al., 2012; Banna et al., 2013;  
44 Bartam and Ballance, 1996). A limit in our understanding of water geochemistry at the  
45 Earth's surface is limited by the temporal resolution at which sampling can be operated  
46 (Whitehead et al., 2009). As summarized by J. Kirchner: "If we want to understand the  
47 full symphony of catchment hydrochemical behaviour, then we need to be able to hear  
48 every note." (Kirchner et al., 2004, page 1358). Yet, taking high-frequency sample sets  
49 back to the laboratory, filtering and analysing them for several elements is limited by  
50 the requirement of considerable human resources (Chapman et al., 1996; Danielsen et

51 al., 2008; Halliday et al., 2015; Neal et al. 2013; Rozemeijer et al., 2014; Strobl and  
52 Robillard, 2008; Telci et al., 2009).

53 A significant number of studies have reported high-frequency chemical measurements  
54 in watersheds. Thus far, these data have been mostly acquired during limited periods of  
55 time such as single storm events or a day (Beck et al., 2009; Brick et al., 1996;  
56 Chapman et al., 1997; Gammons et al., 2007; Kurz et al., 2013; Liu et al., 2007; Morel  
57 et al., 2009; Montety et al., 2011; Neal et al., 2002; Nimick et al., 2011; Nimick et al.,  
58 2005; Takagi et al., 2015; Tercier-Weaber et al., 2009). Although these studies clearly  
59 highlighted the wealth of information provided by sampling rivers at sub-hourly  
60 frequency, they underestimate the legacy of past hydrological episodes (Kirchner 2006;  
61 Jasechko et al., 2016; Rode et al., 2016) and are of limited use when mass budgets are to  
62 be calculated for a typical hydrological cycle.

63 To date, the best combination of high-frequency and long-term monitoring ever  
64 reported for river chemistry is a 7-hourly frequency sampling over 18 months (Neal et  
65 al., 2012). In this study, the authors demonstrate the "act of discovery" permitted by  
66 such sampling scheme, by showing that the high sampling frequency of river  
67 hydrochemistry over sufficiently long time spans reveals patterns related to  
68 hydrological and biological drivers that are imperceptible at lower sampling frequency.  
69 Automated approaches, developed using probes installed directly in the river  
70 (Rozemeijer et al., 2010a; Macintosh et al., 2011; Cassidy and Jordan 2011; Dabakk et  
71 al., 1999; Glasgow et al., 2004; Zhu et al., 2010; Yang et al., 2008) or online  
72 instrumental devices in which continuously pumped water is injected (Rozemeijer et al.,  
73 2010b; Zabiegala et al., 2010; Jordan and Cassidy 2011) are alternatives to sampling  
74 methods requiring human intervention. Several papers have been published over the last  
75 decade reporting existing devices mostly focused on monitoring dissolved N or P and

76 organic matter (Clough et al., 2007; Kunz et al., 2012; Aubert et al., 2013a; Aubert et  
77 al., 2013b, Escoffier et al., 2016). A recent overview of the potential of available  
78 conductivity, dissolved oxygen and carbon dioxide, nutrients, dissolved organic matter,  
79 chlrorophyll and Co in situ probes is given by Rode et al. (2016).

80 A new solution for high-frequency measurement of river chemistry is offered by  
81 bringing the laboratory's measuring devices to the field (the "lab in the field" concept).

82 A Swiss group has recently developed such a system (von Freyberg et al., 2017) by  
83 installing ionic chromatography devices in a hut next to a stream. In this paper, we  
84 present a parallel initiative named the River Lab (RL) and funded by the French  
85 program CRITEX: "Innovative sensors for the temporal and spatial EXploration of the  
86 CRITical Zone at the catchment scale" (<https://www.critex.fr>). This approach, like the  
87 previously published one, overcomes traditional limitations on the number of samples  
88 and avoids several issues related to sample transport, filtration and storage. The RL is  
89 able to perform a complete chemical analysis of all inorganic major anionic and cationic  
90 species in the dissolved load of river water using ion chromatography (IC), with a  
91 frequency of up to one complete measurement every 40 minutes.

92 This article is a proof-of-concept paper that describes the analytical design of the RL  
93 and its performance by evaluating the precision, reproducibility and accuracy of  
94 concentration measurements. The first results from the RL reveal a significant  
95 improvement in reproducibility compared to conventional sampling and analysis  
96 techniques. Leveraging these optimal analytical conditions, the RL is able to reveal  
97 temporal patterns of river chemistry, such as daily concentration variations. The RL  
98 opens thus new opportunities in the field of river chemistry research and environmental  
99 monitoring.

100

## 101 **2 Monitoring site**

102 The RL was installed in the Orgeval, Critical Zone Observatory located 70 km eastward  
103 from Paris, France (<https://gisoracle.irstea.fr/>), a temperate agricultural catchment,  
104 within the Seine river watershed, and part of the French Critical Zone Research  
105 Infrastructure OZCAR (“Observatoires de la Zone Critique, Applications et  
106 Recherche”). Orgeval catchment is one of the most instrumented and documented river  
107 observatories in France, with 50 years of hydrological data (Garnier et al., 2014).  
108 Catchment hydrologic data are available on the ORACLE website  
109 (<https://bdoh.irstea.fr/ORACLE/>).

110 The RL is installed at the outlet of the Avenelles River, a sub-catchment in the Orgeval  
111 watershed. The Avenelles River drains an area of 45 km<sup>2</sup>. The climate is temperate and  
112 oceanic, with cool winters (mean temperature 3°C), warm summers (20°C in average)  
113 and an annual precipitation rate of ~650 mm on average. The Avenelles sub-catchment  
114 sits within the sedimentary carbonate-dominated Paris Basin. The river is perennial,  
115 supplied by groundwater from the Brie aquifer; with water chemistry dominated by  
116 Ca<sup>2+</sup>, SO<sub>4</sub><sup>2-</sup>, HCO<sub>3</sub><sup>2-</sup> and NO<sub>3</sub><sup>-</sup> ions. The water level at the Avenelles gauging station  
117 shows an average daily volumetric flow rate of 0.2 m<sup>3</sup>/s (from 1962 to 2016) with low  
118 water period in summer (0.1 m<sup>3</sup>/s) and flash flood events reaching 10.4 m<sup>3</sup>/s in spring.

119

## 120 **3 Design of the River Lab**

121 The concept of the RL is to pump river water and feed it to a set of physico-chemical  
122 probes and ion chromatography instruments (IC) for a complete analysis of major  
123 dissolved species continuously at high frequency (40 minutes is needed for a complete  
124 analysis). All the instruments of the RL fit into an isolated bungalow of 4-m length by  
125 2.5-m width, kept at 24°C ± 2°C. The RL was designed by IPGP (Institut de Physique

126 du Globe de Paris, France) and IRSTEA (Institut national de Recherche en Sciences et  
127 Technologies pour l'Environnement et l'Agriculture, France) and assembled by Endress  
128 & Hauser (E+H<sup>®</sup>) (Fig. 1). A technical sketch is available in supplementary information  
129 (Fig. S11).

130

131 The RL has been designed around a primary circuit, which pumps the river water at 700  
132 liters per hour. First, the unfiltered river water sampled in the middle of the stream (Fig.  
133 1) continuously supplies an overflow tank where 6 parameters are measured: pH,  
134 conductivity, dissolved O<sub>2</sub>, dissolved organic carbon (DOC), turbidity and temperature.  
135 The water is then released into the river downstream from the RL. The turnover time of  
136 water in this primary circuit is 2 minutes. The turbidity probe is installed upstream of  
137 the overflow tank in a pipe perpendicular to the flow to provide more accurate  
138 measurements. The turbidity and DOC probes benefit from an automatic self-cleaning  
139 every 5 minutes using compressed air. For all probes, the frequency of acquisition is  
140 one measurement per minute. The tank and each probe are hand-cleaned weekly. All  
141 probes are developed and provided by Endress & Hauser (E+H<sup>®</sup>).

142

143 Second, a fraction of water pumped through the primary circuit feeds another circuit  
144 directed toward two IC instruments for the measurement of major dissolved species  
145 concentrations. A filtration system is deployed between the primary circuit and the IC  
146 instruments, consisting of a tangential filter with a 2- $\mu$ m pore size, followed by a 0.2-  
147  $\mu$ m frontal filtration system through cellulose acetate filters (Fig. 1) crucial for the IC  
148 instruments. Cation and anion chromatographs, connected in series, are fed  
149 simultaneously every 40 minutes from the filtered water circuit through a injection  
150 valve. Between two injections, the water in the filtered circuit is constantly renewed (1

151 L per hour). Our tests show that the frequency for a complete and uncontaminated  
152 analyse of cation and anion is actually limited by the filtration device (see part 4.3).  
153 The IC analysis is performed using two Dionex<sup>®</sup> ICS-2100 (Thermo Fisher Scientific<sup>®</sup>)  
154 instruments using eluent produced with concentrated eluent cartridges and ultra-pure  
155 water (Fig. 1). The cationic species measured are Na<sup>+</sup>, K<sup>+</sup>, Mg<sup>2+</sup> and Ca<sup>2+</sup>, and anionic  
156 species are Cl<sup>-</sup>, NO<sub>3</sub><sup>-</sup> and SO<sub>4</sub><sup>2-</sup>. The chosen analysis time is 30 minutes (40 minutes if  
157 Sr<sup>2+</sup> concentration measurements are included; see details in SI “Ion Chromatographs  
158 characteristics”). The multiport valve installed upstream of the ICs allows us to check  
159 the drift of the instruments and the background signal by regular introduction of  
160 calibration solutions and pure distilled water (see section 4). Pure distilled water is  
161 regularly (every two weeks) introduced to check the residual noise. Both cationic and  
162 anionic chromatographs are calibrated every two months using synthetic solutions  
163 mimicking the river chemistry, made from 1000-ppm mono-elemental standard  
164 solutions. Two sets of calibration solutions are prepared, one for anions and the second  
165 for cations. The first solution (called “River x1”) is prepared based on concentrations of  
166 the river water during summer, i.e. with the highest measured concentrations for most  
167 species. In the second solution, these concentrations are doubled (called “River x2”).  
168 Further solutions are produced out of River x1 and x2 through dilution by up to ten-fold  
169 to achieve lower concentrations (“River x0.5; x0.25; x0.1”). The resulting five  
170 calibration solutions cover the entire range of possible natural variability of each species  
171 observed for the Orgeval River, including flood events.

172

173 Data from probes and ICs are collected, merged and updated in a single database in real  
174 time. Data from the gauging station (flow discharge and precipitation level) are  
175 automatically added to the database. Several parameters of the RL can be remotely

176 monitored such as pump activity, pressure, flow and temperature in the primary circuit;  
177 activation of the tangential filtration cleaning system, instrument connection, and  
178 temperature in the bungalow. A set of alarms and sensors controls each key point of the  
179 system. An email is automatically sent in case of dysfunction. Under normal operating  
180 conditions, the RL needs human intervention only once per week.

181

## 182 **4 Analytical performances of the River Lab**

183 RL data acquisition started on the 12<sup>th</sup> of June 2015. The reliability of the system was  
184 assessed through 5 different tests involving IC measurements and the sampling  
185 procedure (accuracy, drift, precision of the whole system, cross-contamination and  
186 reproducibility). We refer to the 3<sup>rd</sup> edition of JCGM 200-2012 (JCGM 2012) for the  
187 terminology used in assessing the performance criteria.

188

### 189 **4.1 Accuracy and instrumental drift**

190 The aim of the RL is to achieve very high-frequency measurements of river chemistry  
191 over long periods of time (pluriannual). To compensate for any long-term drift in the IC  
192 calibration, instruments are calibrated with a new set of solutions every two months or  
193 after each maintenance operation on the IC instruments. However, calibration drift can  
194 occur over timescales shorter than two months, resulting in systematic and / or random  
195 errors in concentration measurements. We evaluated this effect using a set of injections  
196 of the “River x1” solutions, over one week and over two months, (Tab. 1). For all  
197 species measured, no systematic variation was observed in the measured concentration  
198 of the solution “River x1”, showing that at the two timescales, instrumental drift does  
199 not induce any systematic bias on concentration measurements, and that most of the  
200 error is of random nature. Therefore, the standard deviation of the concentration



201 measurements of a given solution can be used as a reliable measure of the error due to  
202 instrumental drift. The measurement error over one week is calculated as the standard  
203 deviation of concentration measurements over 19 injections of solution "River x1"  
204 performed every 8 hours during one week (from the 5<sup>th</sup> to the 12<sup>th</sup> of November 2015).  
205 The measurement error over two months is calculated as the standard deviation of  
206 concentration measurements over a series of injections performed every two days  
207 during two months (from the 28<sup>th</sup> December 2015 to the 26<sup>th</sup> February 2016). These  
208 error estimates are lower than 1 % over one week and lower than 1.7 % over two  
209 months (Tab.1). The agreement between the calculated concentrations of the "River x1"  
210 solution and the RL measurements also demonstrate the accuracy of the prototype (Tab.  
211 1).

212

#### 213 **4.2 Precision of the whole system**

214 In order to estimate the precision of the whole system (IC instruments combined with  
215 the sampling device including the primary circuit, the pump and the filtration units), we  
216 performed a "closed-loop experiment" over the course of one day by connecting the  
217 inlet and the outlet of the primary circuit to a 300-L tank containing river water. The test  
218 was performed three times over two different seasons (the 20<sup>th</sup> of July 2015, the 28<sup>th</sup> of  
219 August 2015, and the 17<sup>th</sup> of April 2016). The conductivity probe (one measurement  
220 every minute) was used to check the stability of the water chemistry during the course  
221 of the experiment (Fig. SI 2). Our results show that a lapse of 2 hours at least is  
222 necessary for the system to stabilize, corresponding to the homogenization time of the  
223 water within the closed loop (Fig. 2). After two hours, major anion and cation  
224 concentrations show a remarkable stability indicating the absence of drift over of 24-  
225 hour time lapse despite the temperature variations in the river water, and allowing us to

226 estimate the precision of the whole system over one day using the standard deviation of  
227 the measurements performed during the test. The results of the test are presented in  
228 Table 2. The precision reached is lower than 0.5% for all species except for potassium,  
229 for which it is lower than 1.2%.

230

### 231 **4.3 Cross-contamination**

232 The ability of the RL to detect rapid variations in river chemistry (typically expected  
233 during storm events) depends on 1) the response time of the RL to a perturbation in the  
234 river and 2) the potential cross contamination from one sample to the next one. We  
235 assessed these two effects by a tracer injection experiment. After establishing a closed-  
236 loop experiment (on the 29<sup>th</sup> of August 2015) and allowing for the period of  
237 stabilization, we introduced a known amount of NaCl (200 g previously dissolved in a  
238 small amount of river water) into the 300-L tank of river water in order to simulate a  
239 “spike” in the river chemistry. The monitoring of conductivity in the primary circuit  
240 allowed us to follow the propagation of the spike injection into the primary circuit while  
241 Cl<sup>-</sup> concentrations measured by the IC every 40 minutes allowed us to follow its  
242 propagation through the filtration devices and IC instruments (Fig. 3). The conductivity  
243 probe shows that the salinity spike is detected very quickly and stabilized after 5  
244 minutes. This indicates that the water in the primary circuit is quickly homogenized (in  
245 agreement with the high flow rate of the primary circuit: 700 l/h). Conversely, the Cl<sup>-</sup>  
246 and Na<sup>+</sup> concentrations only reach the expected concentration at the second IC  
247 measurement i.e. after 80 minutes.

248

249 The first IC measurement following the spike injection indicates that only 93% of the  
250 final steady-state concentration is reached, revealing a contamination of the (n)<sup>th</sup> sample

251 by 7% of the (n-1)<sup>th</sup> sample. In practice, such a contamination will only be significant if  
252 the instantaneous derivative of river concentration with time is important. In the case of  
253 the Orgeval River, where the RL is deployed, the relative derivative of the concentration  
254 with respect to time is lower than 1% per hour for 90% of the time for all species. In  
255 this case, the cross-contamination induces an error of 0.07% compared to the true  
256 concentration, which means that the effect of cross contamination is negligible  
257 compared to the precision of the RL (see section 4.2). However, in the case of flood  
258 events, when the stream flow increases quickly, the derivative of concentration can  
259 change by more than 10% per hour. In such cases, cross contamination will induce an  
260 error of 1% or more. The injection test shows that the time resolution of the RL is  
261 limited by the transfer time of the water between sampling and injection into the IC  
262 instruments. This transfer time of the water in the RL is mainly due to the design of the  
263 filtration system, which may be improved in the future.

264

#### 265 **4.4 Reproducibility: RL vs Laboratory**

266 As a final test for assessing the ability of the RL to record fine natural variations of river  
267 chemistry in comparison to conventional techniques of filtration and analyses in the  
268 laboratory, we focused on two days in the summer of 2015 following long periods  
269 without rain (21<sup>st</sup> of July 2015 for cations and 19<sup>th</sup> of April 2016 for anions) which  
270 showed very high resolution diurnal variations (<5% relative) in chemical composition  
271 of the Orgeval river. In addition to the analyses made by the RL every 40 minutes, we  
272 conducted hourly sampling of the river by collecting 5 litres of water and filtering it  
273 immediately using a Teflon<sup>®</sup> frontal filtration unit (Sartorius<sup>®</sup>) with 0.2- $\mu$ m porosity  
274 polysulfonether filters. Bottles of acidified (at pH = 2) and unacidified river water were  
275 transported to the laboratory at IPGP for measurement of major cations and anions,

276 respectively, using IC devices similar to those installed in the RL (Thermo Fisher<sup>®</sup> ics  
277 2100). In the laboratory, measurements were performed using Thermo Fisher<sup>®</sup> ics 5000  
278 for cations measurements and Dionex<sup>®</sup> 120 from Thermo Fisher<sup>®</sup> for anions  
279 measurements. The calibration procedure in both laboratory and RL is the same using  
280 the same set of calibration solutions. The error measurement reached in the laboratory is  
281 estimated at 1% through repeated injections of the standard solution “River x1” (every 5  
282 samples). Comparison between the RL and the laboratory for the seven measured  
283 species are shown in Figure 4. First, the measurements made by the RL are more precise  
284 than those performed in the laboratory, a feature that can be primarily attributed to the  
285 greater stability of the continuously working injection system of the RL. Second, the  
286 fine variations measured by the RL are reproduced in the laboratory, validating the  
287 observed diurnal variations and supporting the reliability of the RL to detect changes on  
288 the order of a percent within a day. The third observation is that small yet systematic  
289 offsets between the two sets of data exist, up to 3% for Mg. One possible explanation  
290 for this difference is that the filtration procedures differed between the RL and the  
291 manual sampling, which may have led to a discrepancy in the concentration  
292 measurements related to the potential for some elements to be hosted in the colloidal  
293 phase (Dupré et al., 1999). In addition, the most accurate measurements were obtained  
294 with the RL rather than with the laboratory equipment because the RL is continuously  
295 processing solutions with a similar matrix, thereby minimizing memory effects and  
296 cross-contamination that can compromise measurements if widely differing samples are  
297 run successively on the same instrument. These features of the measurement protocol,  
298 representative of most laboratory workflows for hydrochemical measurements, are  
299 likely to lead to inaccuracies. Regardless of the observed discrepancy between the two

300 sets of measurements, we note that variations in concentration recorded by the RL and  
301 measured at the IPGP laboratory have the same amplitudes and are synchronous.

302

## 303 **5. Discussion**

### 304 **5.1 What are the benefits of bringing the lab into the field?**

305 The RL presented above allows us to record continuously, at a high frequency and over  
306 long spans of time, the concentration of 7 major dissolved species in a river system.  
307 Although this is beyond the scope of the present paper, the RL presented here opens  
308 new possibilities for the exploration of the fine structure of hydrochemical evolution at  
309 the catchment scale and for improved understanding of the associated hydrological,  
310 geochemical, and biological processes. From a technical point of view, our study shows  
311 that deploying the conventional laboratory measurement techniques in the field adds  
312 significant value. The tests performed and reported above clearly demonstrate an  
313 improvement in precision compared to the analysis of bottled samples taken back to the  
314 lab. We see three main reasons for this improvement.

315 1) In a given river, dissolved concentrations typically vary by less than one order of  
316 magnitude when water discharge changes by several orders of magnitude (Godsey et al.,  
317 2009). This constancy allows us to select a relatively narrow range of concentration for  
318 establishing specific calibration curves of the IC instruments, a condition which is rarely  
319 possible in the laboratory where different kinds of samples are analyzed.

320 2) While in the laboratory samples are injected discretely, in the RL river water samples  
321 are injected as a continuous flow. Thus, the primary circuit and the filtration system  
322 operate continuously at a constant pressure, which supports stable and accurate  
323 analyses.

324 3) The third factor is the experimental conditions in the bungalow. The temperature is  
325 maintained at  $24^{\circ}\text{C} \pm 2^{\circ}$  (in addition to the  $40^{\circ}\text{C}$  thermostatically-controlled  
326 temperature in the column, precolumn and detection device of the ICs) allowing for  
327 better stability of the IC measurements. Moreover, the RL IC instruments are never  
328 stopped, which favours stability.

329

## 330 **5.2 What is revealed by a higher sampling frequency?**

331 To our knowledge, the high frequency of measurements (one measurement every 40  
332 minutes) reached by the RL installed on the Orgeval River is the highest ever reported  
333 for stream chemistry over several months. To highlight the corresponding improvement  
334 in the recorded concentration signal, we tested the effect of sampling frequency on the  
335 concentration signal. First, we artificially sub-sampled the RL original signal at two  
336 lower sampling frequencies: every 7 hours (starting October 5<sup>th</sup>, 2015 at 10 pm) and  
337 every 24 h. The 7-hourly frequency was chosen to reproduce the sampling frequency of  
338 Neal et al., (2012) made in the Plynlimon watershed, Wales. The daily sampling  
339 frequency is typically what is achievable on the long term by "human grab-sampling" in  
340 the field. Second, we calculated the probability density function (PDF) of concentration  
341 measurements over a given time interval. The use of PDFs allows us to explore the  
342 structure of concentration signals beyond the mean concentration, which constitutes an  
343 important metric for river solute budget, but lacks any insight into the variations in  
344 concentrations that can be used to retrieve information on catchment processes. We  
345 describe the PDF by 3 statistical parameters: mean, standard deviation and skewness.  
346 Skewness indicates the distribution asymmetry, both in magnitude and direction (a  
347 positive skewness means that most values are higher than the mean). Altogether, the  
348 three parameters account, at first-order, for the structure of a concentration signal. We

349 compared these three parameters for the computed PDFs to quantify the signal  
350 degradation induced by artificial sub-sampling.

351 We applied this statistical approach to two representative periods of the hydrological  
352 cycle of the Orgeval Critical Zone Observatory: a typical 6-day rain event caused by the  
353 arrival of a wet, Atlantic meteorological front (in October 2015) and a dry summer low  
354 water stage period (July 2015) where the stream is essentially sustained by groundwater,  
355 during an apparently steady hydrological period. We first present the behaviour of  
356 calcium and sulphate concentrations as an example during the two considered periods  
357 (Fig. 5 and 6), before generalizing to all measured species (Supplementary information  
358 and Fig. SI 3, SI 5 and SI 6).

359

360 **Rain event.** The Ca concentration time series recorded at a 40-minutes frequency shows  
361 that minimum Ca concentrations are recorded at maximum water discharge, but this  
362 relationship is invisible at lower sampling frequency (Fig. 5). Narrow peaks during the  
363 maximum of the stream flow are unresolved at a daily or 7-hourly frequency. The  
364 comparison of the calculated PDF shows that a bimodal character is captured at all  
365 frequencies. The average and standard deviation are not significantly affected by the  
366 sampling frequency, with a relative difference of less than 2% for the values of these  
367 parameters between the three distributions. However, the skewness values vary among  
368 the different records. From the 40-minutes frequency to the daily frequency signals, the  
369 skewness is weaker, which means that even if the overall concentration variability is  
370 well captured at the lower sampling frequencies, the concentration signal is clearly  
371 degraded. This degradation is particularly intense during the middle of the rain event,  
372 where the concentration signal evolves quickly.

373

374 **Summer event.** Despite the absence of rain events during the 2015 summer, the River  
375 Lab recorded high frequency variations revealing a diurnal structure with 7% relative  
376 variations between day and night. Each element exhibits its own type of daily variation  
377 in terms of amplitude and regularity. The Figure 6 shows that the structure of this signal  
378 is altered when the sampling frequency decreases. While these daily variations are still  
379 captured when sampling occurs every 7 hours, their amplitude is somewhat altered (5%)  
380 compared to the 40-minutes sampling frequency (8%). The daily variability of the  
381 signal is absent on the daily sampling frequency. While the mean remains the same over  
382 the range of sampling frequency, the variability quantified by the relative standard  
383 deviation decreases with lower sampling frequency, by up to 50% for the daily  
384 frequency compared to the 40-minutes frequency signal, indicating a significant loss of  
385 information. The skewness of the concentration distribution recorded at a sub-sampled  
386 daily frequency has a value that is opposite in sign compared to the other two  
387 frequencies, indicating that there is an inversion of the measured asymmetry of the PDF  
388 at lower sampling frequencies. Therefore, too coarse of a sampling frequency can yield  
389 a strongly altered signal compared to higher frequencies, resulting in a biased shape of  
390 the distribution of the concentrations.

391

392 **Generalization.** The resampling approach applied above is generalized and expanded to  
393 other elements for both the summer and rain events. The generalization to all species  
394 measured is presented in supplementary information. In Figures 5 and 6, we arbitrarily  
395 chose the hour of sampling (10 a.m. and 2 p.m. for Figures 5 and 6, respectively). In  
396 figure SI 3, SI 5 and SI 6, the sub-sampling is performed at each of the possible  
397 sampling hours. This statistical analysis quantitatively demonstrates that such high  
398 frequency measurements are able to capture the day-night chemical cycles of the



399 Orgeval River. Given the amplitude and duration of typical rain events in the catchment,  
400 the alteration of the signal by lowering the sampling frequency is less critical but still  
401 significant during these periods (Supplementary information; Fig. SI 3, SI 5 and SI 6).

402

### 403 **5.3 What is revealed by better analytical precision?**

404 As shown above, the Orgeval RL not only achieves high-frequency measurements but  
405 also results in improved precision compared to conventional lab analysis following  
406 manual sampling. Therefore, any sampling procedure, even at a high frequency,  
407 involving conventional lab analysis induces a loss of precision. We demonstrate this  
408 effect through a numerically generated artificial degradation of the precision. Using the  
409 original RL concentration signal as a reference, we artificially degraded the signals by  
410 adding a normally distributed noise onto the concentration signals recorded by the RL.  
411 Noise levels of 4% and 2% were tested as they are representative of the “standard”  
412 analytical precision reported for most laboratory IC devices. The same representative  
413 periods as in the previous section (summer and rain events) were utilized for these tests.  
414 In this section we present the example of one element for each characteristic period  
415 ( $\text{Ca}^{2+}$  for rain event Fig. 7 and  $\text{SO}_4^{2+}$  for summer event Fig. 8. The generalization for all  
416 elements is detailed in the supplementary information section (Supplementary  
417 information and Fig. SI 4, SI 7 and SI 8).

418

419 **Rain event.** The Figure 7 illustrates the concentration PDF obtained after degradation  
420 of the analytical precision for the Ca concentration. The narrow peaks recorded during  
421 the maximum of the stream flow are virtually invisible in the signal at a 4%-precision,  
422 and strongly smoothed in the signal at a 2%-precision. The original bimodal  
423 characteristic of the PDF is still visible in the 2%-precision signal but no longer in the

424 4%-precision signal. The mean and standard deviation appear to be insensitive to these  
425 changes in analytical precision, while the skewness is strongly impacted, reflecting  
426 significant alteration of the concentration PDF at lower precision.

427

428 **Summer event.** Figure 8 shows how the sulphate concentration signal is affected when  
429 the precision is degraded. Day-night variations are only visible in the original RL signal  
430 because of its high analytical precision. The effect of degraded precision on the PDFs is  
431 more important than for the rain event (Fig. 7). While the mean value is robust, the  
432 standard deviation is altered (+150% from the RL signal to the 4% precision signal).  
433 The skewness decreases (but keeps the same sign) by up to 90% for the signal at 4%-  
434 precision compared to the original signal and 74% for the signal at 2%-precision,  
435 indicating that the original RL signal asymmetry is lost as precision is worsened. These  
436 changes in the parameters of the concentration PDF show that the structure of the  
437 concentration signal in the Orgeval River would be significantly altered if the  
438 measurements were made with analytical precision lower than that of the RL prototype.

439

440 **Generalization.** This approach has been expanded to other elements for both the  
441 summer and rain events, as shown in the supplementary information, confirming that  
442 concentration PDFs are strongly sensitive to the analytical precision for all species (Fig.  
443 SI 4, SI 7 and SI 8).

444

## 445 **6 Conclusion**

446 This paper demonstrates the feasibility of deploying conventional laboratory  
447 instruments in the field to measure the concentration of major dissolved anions and  
448 cations in rivers ( $\text{Na}^+$ ,  $\text{K}^+$ ,  $\text{Mg}^{2+}$ ,  $\text{Ca}^{2+}$ ,  $\text{Cl}^-$ ,  $\text{SO}_4^{2-}$ ,  $\text{NO}_3^-$ ) at a high frequency (one

449 measurement every 40 minutes) and at a high analytical precision (better than 1%) over  
450 several months. The River Lab prototype was installed in the Avenelles stream at the  
451 Orgeval Critical Zone Observatory, France. The RL features physico-chemical probes,  
452 an on-line 0.2- $\mu\text{m}$  pore size filtration system, and two ionic chromatographic devices,  
453 all installed in a closed, air-conditioned bungalow. The RL is autonomous, remotely  
454 operable and data can be transmitted automatically. Human intervention is required only  
455 once a week. Therefore, the RL also allows for an efficient attribution of human  
456 resources, as well as considerable saving of consumables.

457 A suite of tests performed on the RL to assess quality measurement and to compare  
458 with more conventional "grab sampling" followed by laboratory measurements revealed  
459 only a minor drift in the instrument calibration, leading to improved precision. This  
460 precision is not easily achieved in the laboratory under standard analysis conditions,  
461 showing the benefit of transporting the laboratory devices to the field. The analytical  
462 capabilities of the RL for major dissolved elements could theoretically be extended to  
463 other elements separable by ion chromatography. Preliminary tests demonstrate that  
464 species present in trace amounts in river water (down to the ppb, such as strontium or  
465 lithium) could be measured with the same gain in precision.

466 For this particular prototype, the measurement frequency (every 40 minutes) appears to  
467 be limited by the turnover time of water in the filtered water circuit, which is itself  
468 imposed by the filtration unit. However, the high frequency and high precision of the  
469 RL enabled precise and accurate observations on the fine structure in hydrochemical  
470 time series. Their interpretation is beyond the scope of the present proof-of-concept  
471 paper but the RL is able to capture the abrupt changes in dissolved species  
472 concentrations during a typical 6-days rain event, as well as daily oscillations during a  
473 hydrological steady period of summer drought.

474 Using the high frequency RL signal as a benchmark, it is possible to artificially alter the  
475 sample frequency and the analytical precision and study the resulting effect on the  
476 hydrochemical distribution obtained for characteristic hydrological events. This analysis  
477 shows that in order to retrieve the fine structure of the hydrochemical signal, high  
478 sampling frequency and improved analytical precision are both necessary conditions. To  
479 paraphrase James Kirchner's quote: "If we want to understand the full symphony of  
480 catchment hydrochemical behaviour, then we need to be able to hear every note"  
481 (Kirchner et al., 2004). The improvements made possible by the RL here or  
482 concomitantly by von Freyberg et al. (2017) allow us to consider hearing the full  
483 potamological symphony.

484 Future work will explore the relationships between the desired measurement frequency  
485 and the timescales characterizing the complex interactions between primary and  
486 secondary minerals, biotic processes and hydrological processes in catchments.  
487 Recording such fine stream hydrochemical variations has the potential to offer a new  
488 perspective in Critical Zone Science development.

489

#### 490 **Author's information**

491 Corresponding author: \*E-mail: [floury@ipgp.fr](mailto:floury@ipgp.fr) and [gaillardet@ipgp.fr](mailto:gaillardet@ipgp.fr)

492

#### 493 **Acknowledgment**

494 This work was supported by the EQUIPEX CRITEX programme, (grant # ANR-11-  
495 EQPX-0011, PIs J. Gaillardet and L. Longuevergne) and funding from IRSTEA  
496 (Institut national de Recherche en Sciences et Technologies pour  
497 l'Environnement et l'Agriculture). We thank Magadalena Niska for administrative help.

---

498 We would like to thank X. Zhang, Q. Charbonnier, D. Calmels, P. Louvat, J. Kirchner,  
499 J. Druhan, S. Brantley, B. McDowell and J. Chorover for their help in the field and

500 helpful comments. A. Guerin (IRSTEA), S. Losa (Thermo Fisher), C. Fagot, P. Reignier  
501 and M. Bauer from Endress+Hauser Company are thanked for technical assistance. PF  
502 benefited from a doctorate grant from MESR, France. The Orgeval CZO river basin  
503 belongs to the French National Infrastructure OZCAR (Observatoires de la Zone  
504 Critique, Applications et Recherche).

505

506

507

## 508 **References**

509

510 Aubert, A. H., Gascuel-Oudou, C., Gruau, G., Akkal, N. et al. Solute transport  
511 dynamics in small, shallow groundwater-dominated agricultural catchments: insights  
512 from a high-frequency, multisolute 10 yr-long monitoring study. *Hydrol. Earth Syst.*  
513 *Sci.* 2013a, 17, 1379–1391.

514

515 Aubert, A. H., Gascuel-Oudou, C., Merot P. Annual hysteresis of water quality: A  
516 method to analyse the effect of intra- and inter-annual climatic conditions.  
517 *Journal of Hydrology.* 2013b, 478, 29–39.

518

519 Aubert, A.H., Kirchner, J. W., Gascuel-Oudou, C., Faucheux, M. et al. Fractal Water  
520 Quality Fluctuations Spanning the Periodic Table in an Intensively Farmed Watershed.  
521 *Environ. Sci. Technol.* 2014, 48, 930–937.

522

523 Azzaro F., Galletta M. Automatic colorimetric analyzer prototype for high frequency  
524 measurement of nutrients in seawater . *Marine Chemistry.* 2006, 99, 191–198.

525

526 Bain R., Gundry S., Wright J., Yang H., Pedley S., Bartram J. Accounting for water  
527 quality in monitoring access to safe drinking-water as part of the Millennium  
528 Development Goals: lessons from five countries. *Bull World Health Organ.* 2012, 90,  
529 228–235.

530

531 Banna M., Imran S., Francisque A., Najjaran H., Sadiq R., Rodriguez M., Hoofar M.  
532 Online Drinking Water Quality Monitoring: Review on Available and Emerging  
533 Technologies. *Environ. Sci. Technol.* 2014, 44, 1370-1421.

534

535 Bartram J., Ballance R. Water Quality Monitoring. A practical guide to the design and  
536 implementation of freshwater quality studies and monitoring programmes. *United*  
537 *Nations Environment Programme.* 1996, 400 pages.

538

539 Beck A. J., Janssen F., Polerecky L., Herlory O., De Beer D. Phototrophic Biofilm  
540 Activity and Dynamics of Diurnal Cd Cycling in a Freshwater Stream. *Environ. Sci.*  
541 *Technol.* 2009, 43, 7245–7251.  
542

543 Brick, CM., Moore J. N. Diel variation of trace metals in the upper Clark Fork River,  
544 Montana. *Environ Sci Technol* .1996, 30, 1953–1960.  
545

546 Calmels D., Galy A., Hovius N., Bickle M., West A., Chen M., Chapman H.  
547 Contribution of deep groundwater to the weathering budget in a rapidly eroding  
548 mountain belt, Taiwan. *Earth and Planetary Science Letters*. 2011, 303 48–58.  
549

550 Cassidy R., Jordan P. Limitations of instantaneous water quality sampling in surface-  
551 water catchments: Comparison with near-continuous phosphorus time-series data.  
552 *Journal of Hydrology*, 2011, 405, 182–193.  
553

554 Chan E. , Kessler J., Shiller A., Joung D., Colombo F. Aqueous Mesocosm Techniques  
555 Enabling the Real-Time Measurement of the Chemical and Isotopic Kinetics of  
556 Dissolved Methane and Carbon Dioxide. *Environ. Sci. Technol.* 2016, 50, 3039–3046.  
557

558 Chapman D. Water Quality Assessments - A Guide to Use of Biota, Sediments and  
559 Water in Environmental Monitoring - Second Edition. *United Nations Environment*  
560 *Programme*, 1996, 651 pages.  
561

562 Chapman, P. J., Reynolds, B., Wheeler, H. S. Sources and controls of calcium and  
563 magnesium in storm runoff: the role of groundwater and ion exchange reactions along  
564 water flowpaths. *Hydrol Earth Syst Sci.* 1997, 1, 671–685.  
565 283, 3–17.  
566

567 Clough T., Buckthought L., Kelliher F., Sherlock R. Diurnal fluctuations of dissolved  
568 nitrous oxide (N<sub>2</sub>O) concentrations and estimates of N<sub>2</sub>O emissions from a spring-fed  
569 river: implications for IPCC methodology. *Global Change Biology*. 2007. 13, 1016–  
570 1027.  
571

572 Dåbakk E., Nilsson M., Geladi P., Wold S., Renberg I. Sampling reproducibility and  
573 error estimation in near infrared calibration of lake sediments for water quality  
574 monitoring. *Journal of Near Infrared Spectroscopy*, 1999 , 7, 241–250.  
575

576 Danielsen F., Burgess N. et al. Local Participation in Natural Resource Monitoring: a  
577 Characterization of Approaches. *Conservation Biology*, 2008, 23, 31–42.  
578

579 de Montety, V., Martin, J.B., Cohen, M.J., Foster, C., Kurz, M.J., Influence of diel  
580 biogeochemical cycles on carbonate equilibrium in a karst river. *Chemical Geology*.  
581 2011, 283, 31–43.  
582

583 Dupré B., Viers J., Dandurand J.L., Polve M., Bénézech P., Vervier P., Braun J.J.. Major  
584 and trace elements associated with colloids in organic-rich river waters: ultrafiltration of  
585 natural and spiked solutions. *Chemical Geology*, 1999, 160, 63-80.  
586

587 Escoffier, N., Bensoussan, N., Vilmin, L., Flipo, N., Rocher, V., David, A., ... &  
588 Groleau, A. (2016). Estimating ecosystem metabolism from continuous multi-sensor  
589 measurements in the Seine River. *Environmental Science and Pollution Research*, 1-17.  
590

591 Feng, X. H., Kirchner, J. W., Neal, C. Measuring catchment-scale chemical retardation  
592 using spectral analysis of reactive and passive chemical tracer time series. *Journal of*  
593 *Hydrology*. 2004, 292, 296–307.  
594

595 Gammons, C. H., Grant T. M., Nimick, D. A., Parker, S. R., DeGrandpre, M. D. Diel  
596 changes in water chemistry in an arsenic-rich stream and treatment-pond system.  
597 *Science of the Total Environment*. 2007, 384, 433–451.  
598

599 Garnier J., Billen, G., Vilain, G., Benoit, M., Passy, P., Tallec, G., Tournebize, J., et al.  
600 Curative vs. preventive management of nitrogen transfers in rural areas: Lessons from  
601 the case of the Orgeval watershed (Seine River basin, France). *Journal of*  
602 *Environmental Management*. 2014, 144, 125–134.  
603

604 Glasgow H., Burkholder J., Reed R., Lewitus A., Kleinman J. Real-time remote  
605 monitoring of water quality: a review of current applications, and advancements in  
606 sensor, telemetry, and computing technologies. *Journal of Experimental Marine*  
607 *Biology and Ecology*, 2004, 300, 409–448.  
608

609 Halliday S., Skeffington R., Wade A., Bowes M., Gozzard E., Newman J., Loewenthal  
610 M., Palmer-Felgate E., Jarvie H. High-frequency water quality monitoring in an urban  
611 catchment: hydrochemical dynamics, primary production and implications for the Water  
612 Framework Directive. *Hydrological Processes*. 2015, 29, 3388–3407.  
613

614 Huang K., Cassar N., Jonsson B., Cai W., Bender M. An Ultrahigh Precision, High-  
615 Frequency Dissolved Inorganic Carbon Analyzer Based on Dual Isotope Dilution and  
616 Cavity Ring-Down Spectroscopy. *Environ. Sci. Technol.* 2015, 49, 8602–8610.  
617

618 Jasechko, S., Kirchner, J. W., Welker, J. M., McDonnell, J. J. Substantial proportion of  
619 global streamflow less than three months old. *Nature Geoscience*. 2016, 9, 126–130.  
620

621 JCGM 200:2012. International vocabulary of metrology – Basic and general concepts  
622 and associated terms (VIM). 2012.  
623

624 Jones T., Chappell N., Tych W. First Dynamic Model of Dissolved Organic Carbon  
625 Derived Directly from High-Frequency Observations through Contiguous Storms.  
626 *Environ. Sci. Technol.* 2014, 48, 13289–13297.  
627

628 Jordan P., Cassidy R. Technical Note: Assessing a 24/7 solution for monitoring water quality loads in  
629 small river catchments. *Hydrol. Earth Syst. Sci.*, 2011, 15, 3093–3100.  
630

631 Kirchner, J. W., Feng, X., Neal, C. Fractal stream chemistry and its implications for  
632 contaminant transport in catchments. *Nature* 2000, 403, 524–527.  
633

634 Kirchner, J. W., Feng, X., Neal, C. Catchment-scale advection and dispersion as a  
635 mechanism for fractal scaling in stream tracer concentrations. *J Hydrol.* 2001, 254, 81-  
636 100.

637  
638 Kirchner, J. W., Feng, X., Neal, C., Robson, A. J. The fine structure of water-quality  
639 dynamics: the (high-frequency) wave of the future. *Hydrological Processes*. 2004, 18,  
640 1353–1359.

641  
642 Kirchner, J. W. Getting the right answers for the right reasons: Linking measurements,  
643 analyses, and models to advance the science of hydrology. *Water Resour. Res.* 2006, 42,  
644 1–5.

645  
646 Kurz, M. J., de Montety, V., Martin, J. B., Cohen, M. J., Foster, C. R. Controls on diel  
647 metal cycles in a biologically productive carbonate-dominated river. *Chemical Geology*.  
648 2013, 358, 61–74.

649  
650 Liu, Z., Liu, X., Liao, C., Daytime deposition and nighttime dissolution of calcium  
651 carbonate controlled by submerged plants in a karst spring-fed pool: insights from high  
652 time-resolution monitoring of physico-chemistry of water. *Environ Geol.* 2008, 55,  
653 1159–1168.

654  
655 Macintosh K., Jordan P., Cassidy R., Arnscheidt J., Ward C. Low flow water quality in  
656 rivers, septic tank systems and high-resolution phosphorus signals. *Science of the Total  
657 Environment*, 2011, 412, 58–65.

658  
659 Morel, B., Durand, P., Jaffrezic, A., Gruau, G., Molenat, J. Sources of dissolved  
660 organic carbon during storm flow in a head-water agricultural catchment, *Hydrological  
661 Processes*. 2009, 23, 2888–2901.

662  
663 Neal, C., Watts, C., Williams, R. J., Neal, M., Hill, L., Wickham, H. Diurnal and longer  
664 term patterns in carbon dioxide and calcite saturation for the River Kennet, south-  
665 eastern England. *The Science of the Total Environment*. 2002, 205–231.

666  
667 Neal, C., Reynolds, B., Norris, D., Kirchner, J. W., Neal, M., Rowland, P., et al. Three  
668 decades of water quality measurements from the Upper Severn experimental catchments  
669 at Plynlimon, Wales: an openly accessible data resource for research, modelling,  
670 environmental management and education. *Hydrological Processes*. 2011. 25, 3818–  
671 3830.

672  
673 Neal, C., Reynolds, B., Rowland, P., Norris, D., Kirchner, J. W., Neal, M., Sleep, D.,  
674 Lawlor, A., Woods, C., Thacker, S., Guyatt, H., Vincent, C., Hockenhull, K., Wickham,  
675 H., Harman, S., Armstrong, L. High-frequency water quality time series in precipitation  
676 and streamflow: From fragmentary signals to scientific challenge. *Sci. Total Environ.*  
677 2012, 434, 3–12.

678  
679 Neal, C; Reynolds, B; Kirchner, J. W.; Rowland, P; Norris, D; Sleep, D; Lawlor, A;  
680 Woods, C; Thacker, S; Guyatt, H; Vincent, C; Lehto, K; Grant, S; Williams, J; Neal, M;  
681 Wickham, H; Harman, S; Armstrong, L. High- frequency precipitation and stream water  
682 quality time series from Plynlimon, Wales: an openly accessible data resource spanning  
683 the periodic table. *Hydrological Processes*, 2013, 27, 2531-2539.

684



685 Nimick, D. A., Cleasby, T. E., McCleskey, R. B. Seasonality of diel cycles of dissolved  
686 trace metal concentrations in a Rocky Mountain stream. *Environ Geol.* 2005, 47, 603–  
687 614.

688

689 Nimick, D. A., Gammons, C. H. , Parker, S. R. Diel biogeochemical processes and their  
690 effect on the aqueous chemistry of streams: A review. *Chemical Geology.* 2011, 283, 3-  
691 17.

692

693 Rode, M., Wade, A.J., Cohen, M.J., Hensley, R.T., Bowes, M.J., Kirchner, J.W.,  
694 Arhonditsis, G.B., Jordan, P., Kronvang, B., Halliday, S.J., Ske, R.A., Rozemeijer, J.C.,  
695 Aubert, A.H., Rinke, K., 2016. Sensors in the Stream : The High-Frequency Wave of  
696 the Present. *Environ. Sci. Technol.* 2016, 50, 10297–10307.

697

698 Rozemeijer J., Klein J. , Broers H., van Tol-Leenders T., van der Grift B. Water quality  
699 status and trends in agriculture-dominated headwaters, a national monitoring network  
700 for assessing the effectiveness of national and European manure legislation in The  
701 Netherlands. *Environ Monit Assess*, 2014, 186, 8981–8995.

702

703 Rozemeijer J., van der Velde Y., van Geer F., Bierkens M., Broers H. Direct  
704 measurements of the tile drain and groundwater flow route contributions to surface  
705 water contamination: From field-scale concentration patterns  
706 in groundwater to catchment-scale surface water quality. *Environmental Pollution*,  
707 2010, 158, 3571-3579.

708

709 Rozemeijer J., van der Velde Y., de Jonge H., van Geer F., Broers H., Bierkens M.  
710 Application and Evaluation of a New Passive Sampler for Measuring Average Solute  
711 Concentrations in a Catchment Scale Water Quality Monitoring Study. *Environ. Sci.*  
712 *Technol.* 2010, 44, 1353–1359.

713

714 Strobl R., Robillard P. Network design for water quality monitoring of surface  
715 freshwaters: A review. *Journal of Environmental Management*, 2008, 87, 639–648.

716

717 Takagi, M. Water chemistry of headwater streams under storm flow conditions in  
718 catchments covered by evergreen broadleaved forest and by coniferous plantation  
719 Landscape Ecol Eng. 2015, 11, 293–302.

720

721 Telci I., Nam K., Guan J., Aral M. Optimal water quality monitoring network design for  
722 river systems. *Journal of Environmental Management*, 2009, 90, 2987–2998.

723

724 Tercier-Waeber M., Hezard T., Masson M., Schäfer J. In Situ Monitoring of the Diurnal  
725 Cycling of Dynamic Metal Species in a Stream under Contrasting Photobenthic Biofilm  
726 Activity and Hydrological Conditions. *Environ. Sci. Technol.* 2009, 43, 7237–7244.

727

728 Vuillemin R., Le Roux D., Dorval P., Bucas K., Sudreau J. P., Hamon M., Le Gall C.,  
729 Sarradin P. M. CHEMINI: A new in situ CHEmical MINIaturized analyzer. *Deep-Sea*  
730 *Research I.* 2009, 56, 1391–1399.

731

732 von Freyberg, J., Studer, B., and Kirchner, J. W.: A lab in the field: high-frequency  
733 analysis of water quality and stable isotopes in streamwater and precipitation, *Hydrol.*  
734 *Earth Syst. Sci. Discuss.*, 2017 doi:10.5194/hess-2016-585.

735  
736 Wang Z., Sonnichsen F., Bradley A., Hoering K., Lanagan T., Chu S., Hammar T.,  
737 Camilli R. In Situ Sensor Technology for Simultaneous Spectrophotometric  
738 Measurements of Seawater Total Dissolved Inorganic Carbon and pH. *Environ. Sci.*  
739 *Technol.* 2015, 49, 4441–4449.  
740  
741 Whitehead P., Wilby R., Battarbee R., Kerman M., Wade A. A review of the potential  
742 impacts of climate change on surface water quality. *Hydrological Sciences–Journal–des*  
743 *Sciences Hydrologiques*, 2009, 54, 101-121.  
744  
745 Yang W., Nan J., Sun D. An online water quality monitoring and management system  
746 developed for the Liming River basin in Daqing, China. *Journal of Environmental*  
747 *Management*, 2008, 88, 318–325.  
748  
749 Zabiegała B., Kot-Wasik A., Urbanowicz M., Namieśnik J. Passive sampling as a tool  
750 for obtaining reliable analytical information in environmental quality monitoring. *Anal*  
751 *Bioanal Chem*, 2010, 396, 273–296.  
752 Kunz A., Steinmetz R., Damasceno S., Coldebela A. Nitrogen removal from swine  
753 wastewater by combining treated effluent with raw manure. *Sci. Agric.*, 2012, 69, 352-  
754 356.  
755  
756 Zhu X., Li D., He D., Wang J., Ma D., Li F. A remote wireless system for water quality  
757 online monitoring in intensive fish culture. *Computers and Electronics in Agriculture*,  
758 2010, 71, 3–9.  
759  
760  
761  
762  
763  
764  
765  
766  
767  
768  
769  
770  
771  
772  
773  
774  
775  
776  
777  
778  
779  
780  
781  
782  
783  
784

785 **Table Captions**

786 **Table 1. Assessment of the RL accuracy and instrumental drift based on**  
787 **concentration measurements made after several injections of the standard solution**  
788 **"River x1". The uncertainty on the calibration solution is the quadratic sum of the**  
789 **uncertainty on the standard solutions (provided by the manufacturer) and the**  
790 **overall uncertainty for weighing during solution preparation. Measurement errors**  
791 **over one week and over two months are expressed as the relative standard**  
792 **deviation (RSD) calculated for repeated injections of the solution "River x1"**  
793 **directly into the IC instruments via the multiport valve (see Fig. 1).**

794  
795  
796 **Table 2. Precision on concentration measurements of the whole RL system**  
797 **calculated as the relative standard deviation (RSD) of concentration measurements**  
798 **made over three 24-hour closed loop experiments, during which the inlet and the**  
799 **outlet of the primary circuit are connected through a 300-L tank of river water.**

800  
801  
802  
803  
804  
805  
806  
807  
808  
809  
810  
811  
812  
813  
814  
815  
816  
817  
818  
819  
820  
821  
822  
823  
824  
825  
826  
827  
828  
829  
830  
831  
832  
833

834 **Figure Captions**

835

836

837 **Figure 1. Sketch of the Orgeval River Lab. Bold blue arrows indicate the primary**  
838 **circuit of unfiltered water. Dashed arrows indicate filtered water supplied to IC**  
839 **instruments. 1: The inlet of the primary circuit samples the river at a constant 20-**  
840 **cm depth maintained by buoys. Water is first filtered through a < 2 mm pore size**  
841 **strainer. The distance between the mouth and the pump is 6 m. The primary**  
842 **circuit assembly is almost entirely composed of polyvinyl chloride (PVC) pipes. 2:**  
843 **The electric pump runs continuously at a constant power, leading to a rate of 700**  
844 **liters per hour. 3: Almost all the river water just flows through the pipe and**  
845 **remains unfiltered. A fraction is filtered through a 2  $\mu\text{m}$  tangential stainless steel**  
846 **filtration unit, then filtered through a 0.2  $\mu\text{m}$  cellulose acetate frontal filter prior to**  
847 **being delivered to IC instruments at a flow rate of 1 liter per hour. 4: A multiport**  
848 **valve before introduction to the IC instruments allows for switching between**  
849 **filtered river water and standard or blank solutions. 5: All probes are deployed in**  
850 **an overflow tank of 5 liters of unfiltered river water. 6: The outlet of the primary**  
851 **circuit is downstream in the river.**

852

853

854 **Figure 2. Assessment of the precision (in deviation from the mean for 4 dissolved**  
855 **species) of the whole RL system including the primary circuit, filtration systems**  
856 **and IC instruments (April, 17<sup>th</sup>, 2016). A closed system is established on the**  
857 **primary circuit of the RL by connecting the inlet and the outlet through a 300-L**  
858 **tank of river water. The system is then run for a period of 24 hours. The time**  
859 **between two IC analyses is 40 minutes. The purple curve represents data of**  
860 **temperature of the water in the tank. We do not consider the 2 first hours (3 first**  
861 **measurements), corresponding to the homogenization of water in the circuit and**  
862 **tank (see conductivity measurements in Fig. SI 2) for the calculation of precision.**

863

864

865 **Figure 3. Cross-contamination assessment and response time of the RL system**  
866 **after a spike injection of 200 of NaCl. A closed system is established on the**  
867 **primary circuit of the RL by connecting the inlet and outlet through a 300-L tank**  
868 **of river water prior to the injection. The conductivity measurement frequency is 1**  
869 **per minute, whereas the time between two measurements of chloride concentration**  
870 **is 40 minutes. Error bars for conductivity and Cl<sup>-</sup> concentration measurements are**  
871 **within symbols size. Results are normalized to the difference between the**  
872 **minimum value, before the tracer injection (0%) and the maximum value, at the**  
873 **end of the experiment (100%).**

874

875

876

877 **Figure 4. Reproducibility assessment of IC measurements made by the RL every**  
878 **40 minutes (blue), compared with concentration measurements made in the**  
879 **laboratory after conventional hourly river sampling (orange). Tests were**  
880 **performed on July 21<sup>st</sup>, 2015 and April 19<sup>th</sup>, 2016 for the cationic and ionic species**  
881 **respectively. For measurements performed in the laboratory, the error**  
882 **measurement is 1% (except for K<sup>+</sup> at 2%) calculated as the standard deviation**

883 over repeated injection of the standard solutions “River x1”. For RL  
884 measurements the error is given in Table 2.  
885

886  
887 **Figure 5. Calcium concentration and stream flow in the Orgeval river during a**  
888 **rain event (from 1 to 25 October 2015), sampled every 40 minutes (RL original**  
889 **signal at 40-minutes frequency) and artificially sub-sampled every 7 hours and**  
890 **every day at 10 a.m. Black dots represent data during the rain event strictly (from**  
891 **5 to 10 October 2015 at 10 a.m.), over which probability density functions (PDFs)**  
892 **of concentration are calculated and represented as histograms (right panels). For**  
893 **each PDF, the following statistical parameters are calculated: average (Ave.),**  
894 **standard deviation (Std D.), and skewness (Skew.). Gray dots represent**  
895 **concentration values outside of the rain event and are not considered in the**  
896 **corresponding PDF. The two statistical parameters standard deviation (Std D.)**  
897 **and skewness (Skew.) are not calculated for the daily subsampling because of the**  
898 **too small number of points.**  
899

900  
901 **Figure 6. Sulphate concentration in the Orgeval river during a summer event**  
902 **(from 7 to the 19 July 2015) sampled every 40 minutes (RL original signal) and**  
903 **artificially sub-sampled every 7 hours, and every day at 2 p.m.. Probability density**  
904 **functions (PDF) of concentration are represented as histograms (right panels). For**  
905 **each PDF, the following statistical parameters are calculated: average (Ave.),**  
906 **standard deviation (Std D.), and skewness (Skew.).**  
907

908  
909 **Figure 7. Calcium concentration and stream flow in the Orgeval river during a**  
910 **rain event (from 1 to the 25 October 2015), as recorded by RL and for two**  
911 **artificially degraded signals using a normally distributed noise with standard**  
912 **deviation of 2% and 4%, to reflect the effect of decreased analytical precision.**  
913 **Black dots represent data during the rain event strictly from 5 (12 a.m.) to 10**  
914 **October 2015. The probability density functions (PDF) of concentration are**  
915 **calculated and represented as histograms (right panels). For each PDF, the**  
916 **following statistical parameters are calculated: average (Ave.), standard deviation**  
917 **(Std D.) and skewness (Skew.). Gray dots represent concentration values outside of**  
918 **the rain event, which are not considered for the analysis presented on the right**  
919 **panels.**  
920

921  
922 **Figure 8. Sulphate concentration in the Orgeval river recorded by the RL during**  
923 **two weeks in summer (7 to 19 July 2015), and for two artificially degraded signals,**  
924 **using a normally distributed noise with a standard deviation of 2% and 4%, to**  
925 **reflect the effect of degraded analytical precision. The probability density**  
926 **functions (PDF) of concentration are calculated and represented as histograms**  
927 **(right panels). The average (Ave.), standard deviation (Std D.), and skewness**  
928 **(Skew.) are calculated for each PDF.**  
929

930

Figure 1

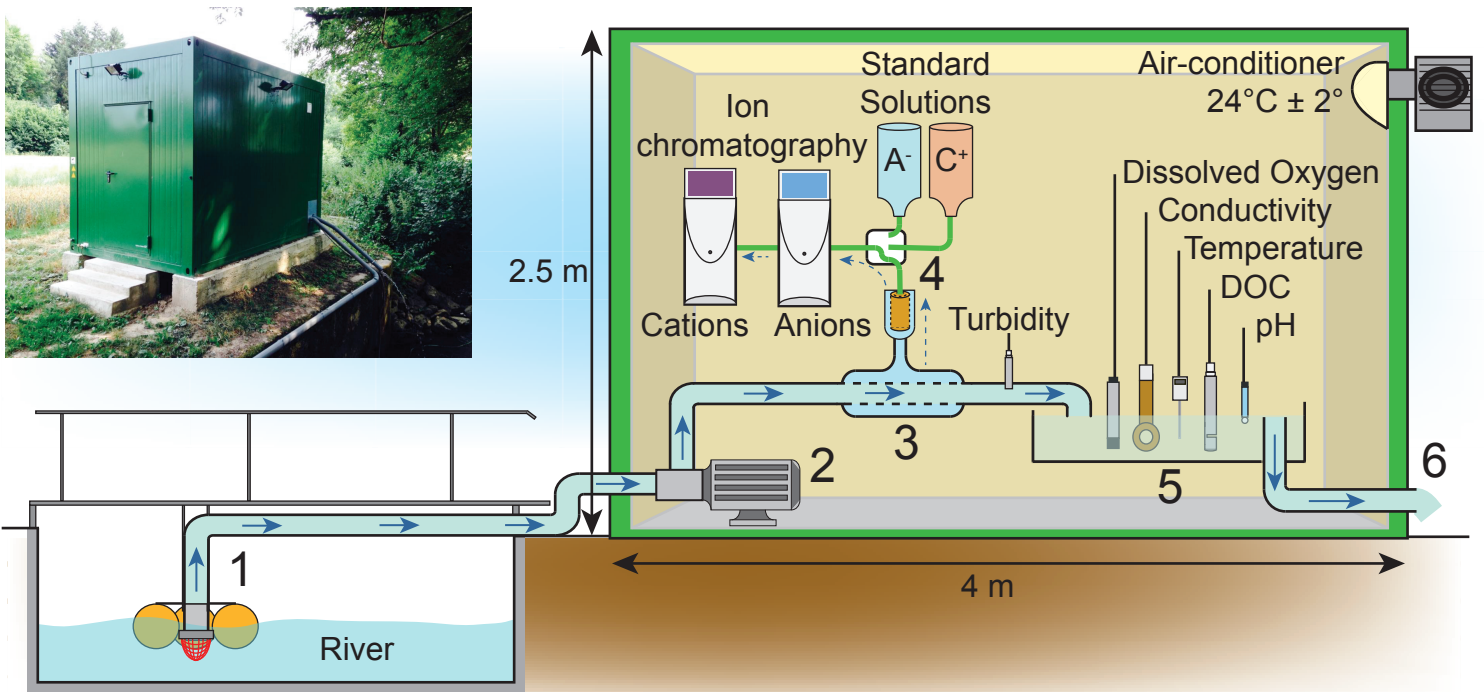


Figure 2

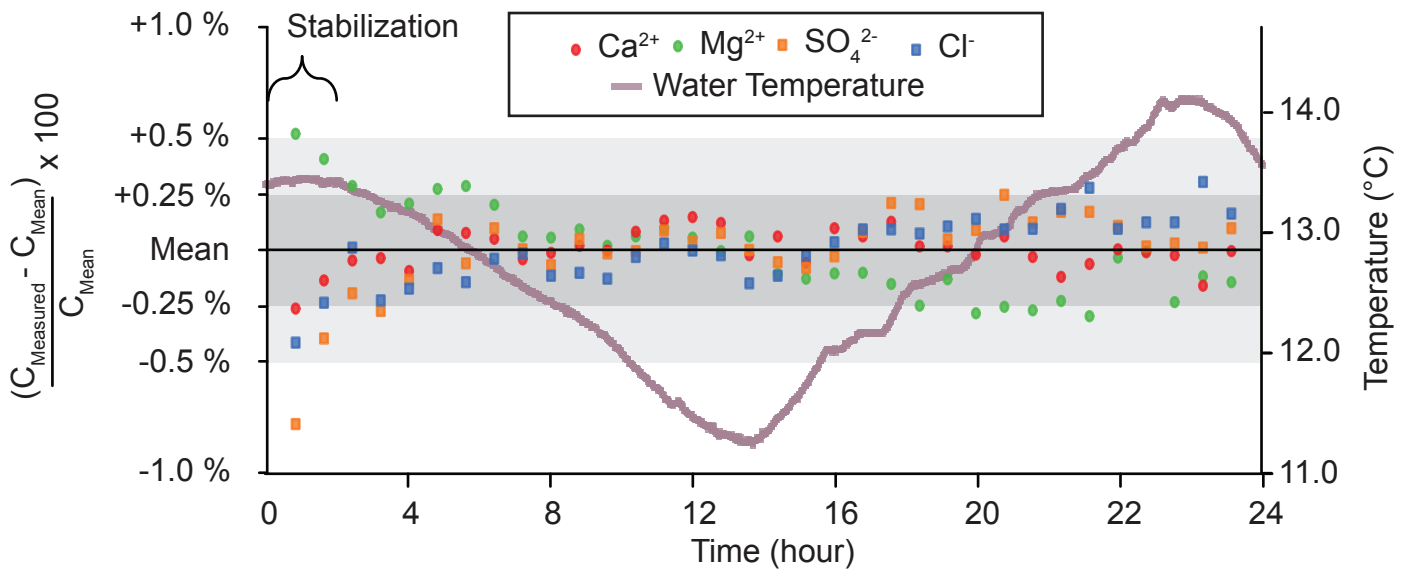


Figure 3

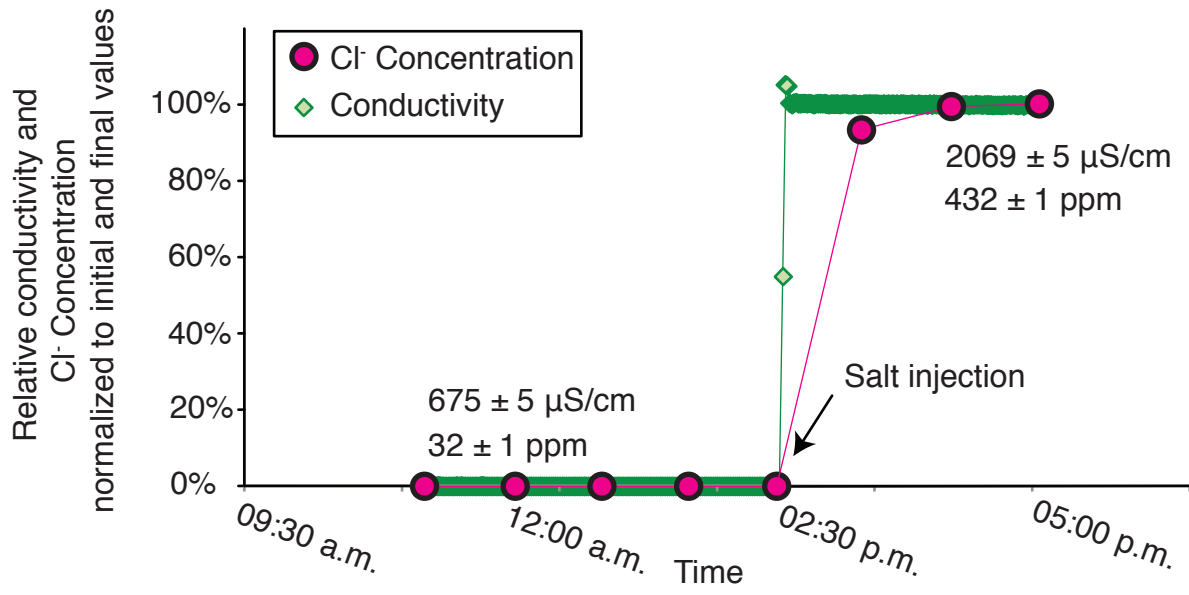




Figure 4

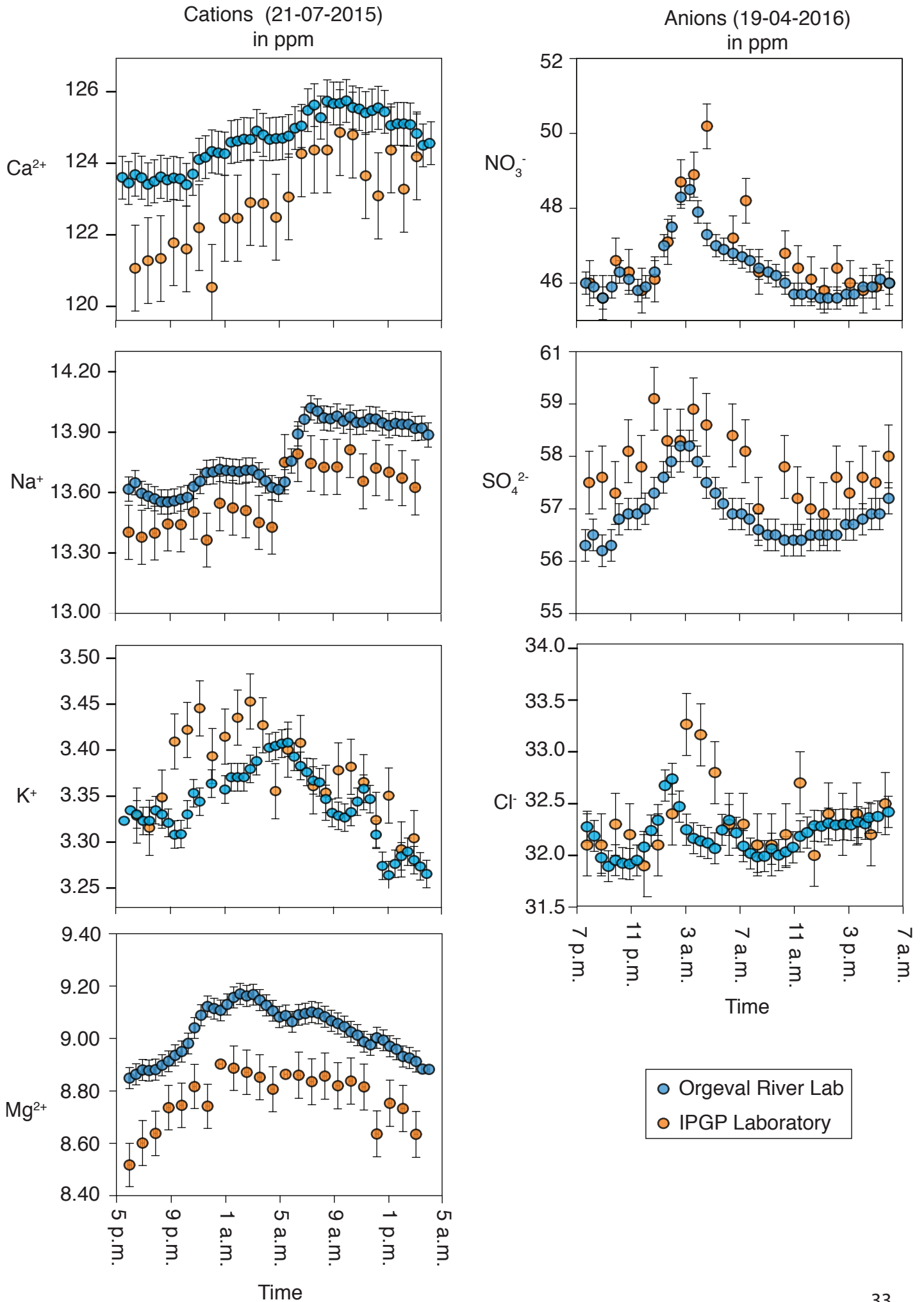
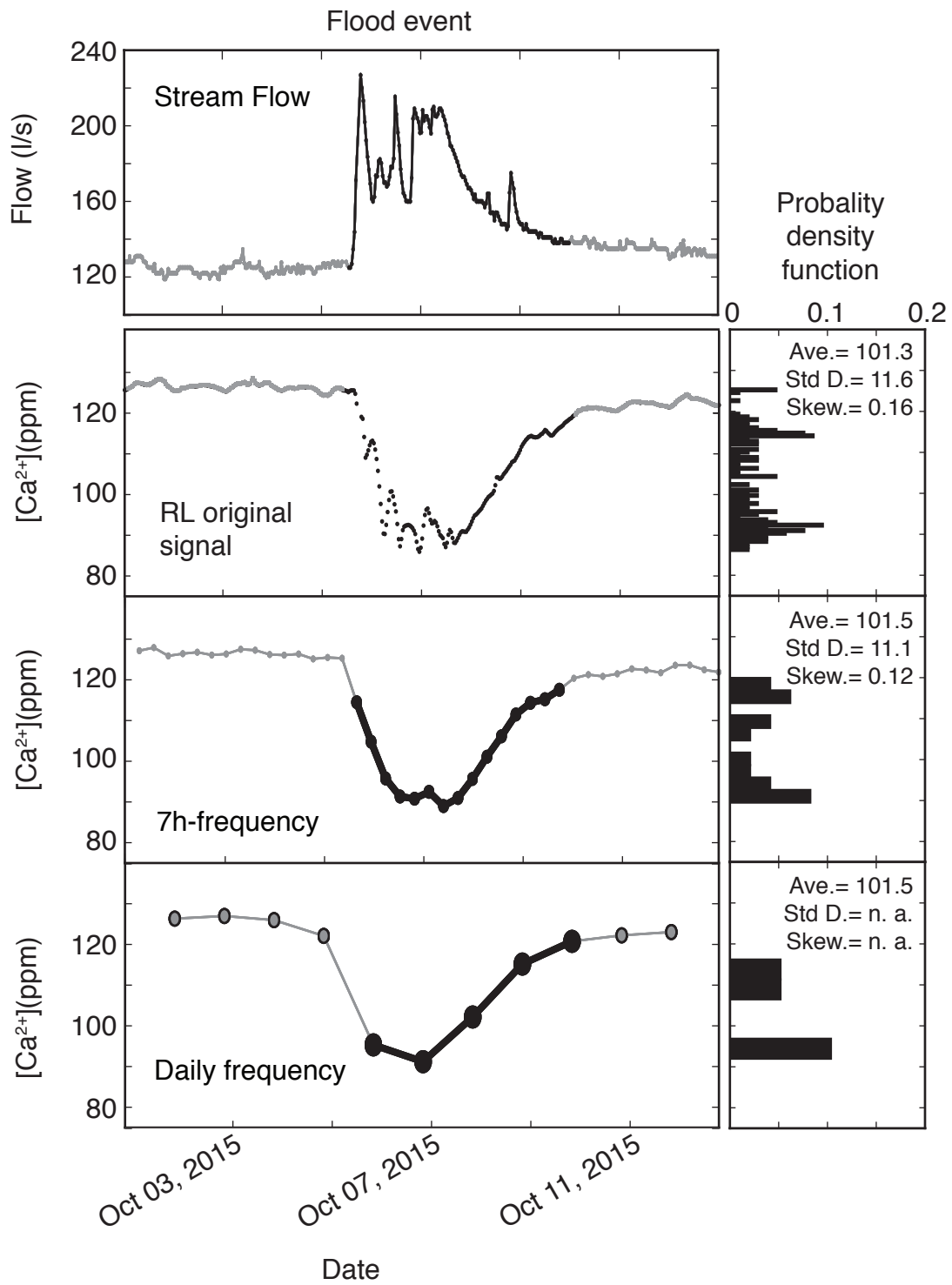


Figure 5



# Summer event

# Probability density function

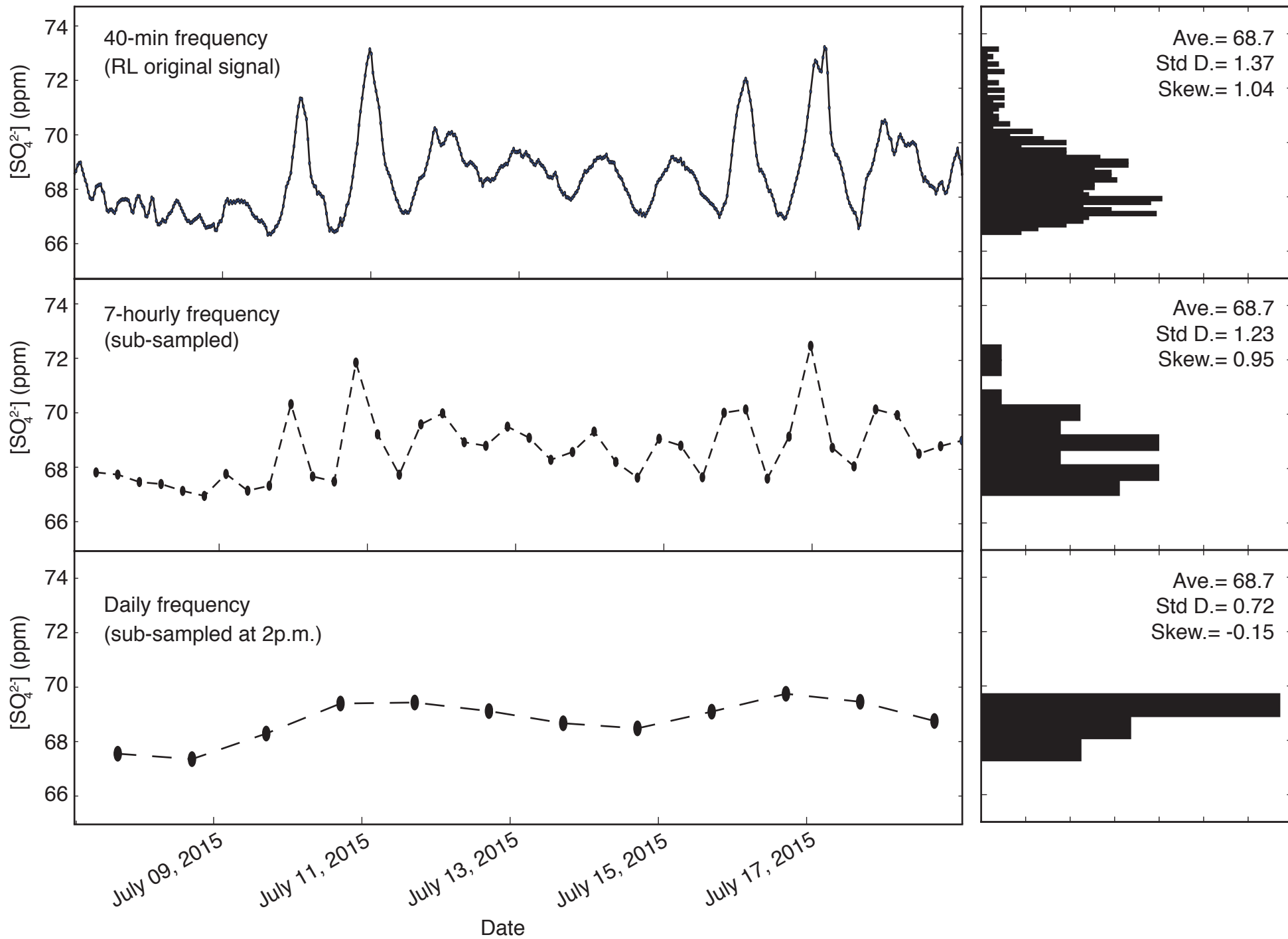
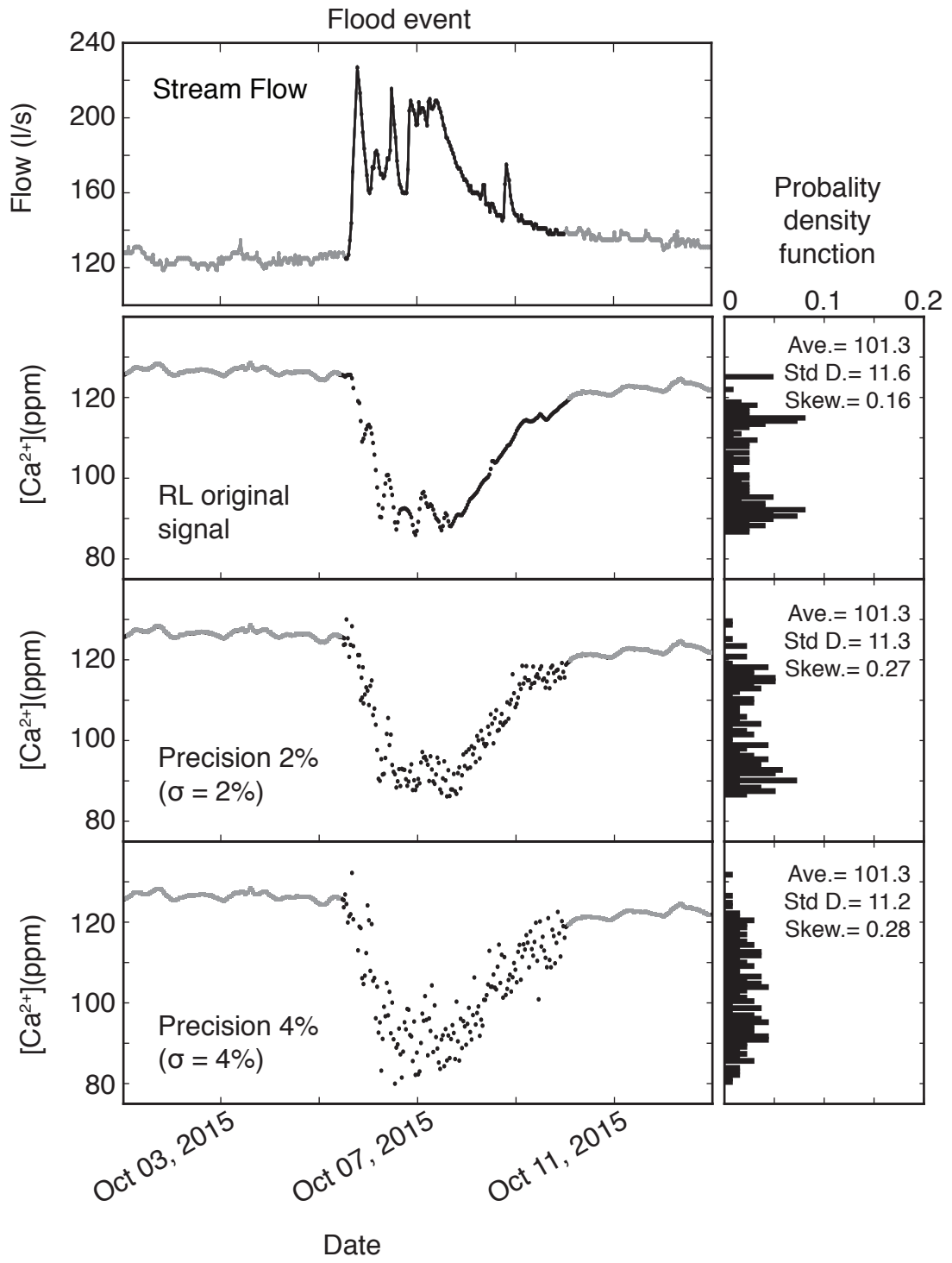


Figure 6

Figure 7



Summer event

Probability density function

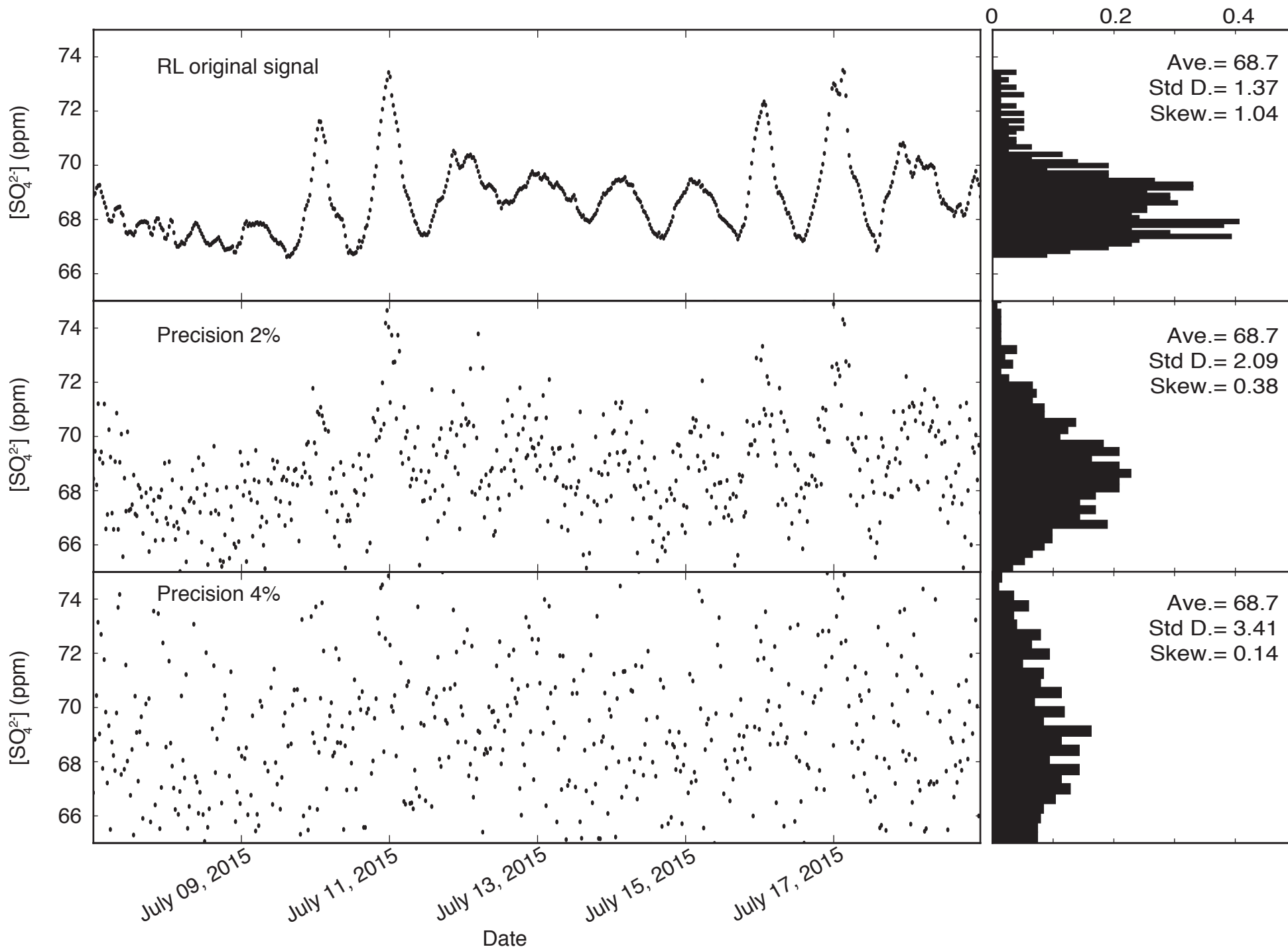


Figure 8

Table 1

	Mg <sup>2+</sup>	K <sup>+</sup>	Ca <sup>2+</sup>	Na <sup>+</sup>	SO <sub>4</sub> <sup>2-</sup>	NO <sub>3</sub> <sup>-</sup>	Cl <sup>-</sup>
Calibration Concentration	10.0	3.0	130.0	10.0	70.0	60.0	40.0
Uncertainty (mg.L <sup>-1</sup> )	0.03	0.01	0.39	0.03	0.84	0.84	0.28
<b>Uncertainty (%)</b>	<b>0.3</b>	<b>0.45</b>	<b>0.3</b>	<b>0.3</b>	<b>1.2</b>	<b>1.4</b>	<b>0.7</b>
<b>One Measurement (Injection of "River x1" solution 4 times successively)</b>							
Number of measurements	(4)	(4)	(4)	(4)	(4)	(4)	(4)
Average (mg.L <sup>-1</sup> )	10.08	3.00	129.86	9.98	70.26	60.31	40.32
SD (mg.L <sup>-1</sup> )	0.02	0.01	0.16	0.02	0.69	0.63	0.27
<b>RSD (%)</b>	<b>0.16</b>	<b>0.27</b>	<b>0.12</b>	<b>0.21</b>	<b>0.86</b>	<b>0.74</b>	<b>0.33</b>
<b>One Week (Injection of "River x1" solution every 8h)</b>							
Number of measurements	(19)	(19)	(19)	(19)	(19)	(19)	(19)
Average (mg.L <sup>-1</sup> )	10.13	3.02	130.64	10.01	70.54	60.63	40.44
SD (mg.L <sup>-1</sup> )	0.03	0.01	0.39	0.02	0.67	0.44	0.22
<b>RSD (%)</b>	<b>0.28</b>	<b>0.32</b>	<b>0.30</b>	<b>0.22</b>	<b>0.96</b>	<b>0.72</b>	<b>0.54</b>
<b>Two months (Injection of "River x1" solution every 2 days)</b>							
Number of measurements	(28)	(28)	(28)	(28)	(25)	(25)	(25)
Average (mg.L <sup>-1</sup> )	10.33	3.14	134.34	10.05	70.05	62.33	40.57
SD (mg.L <sup>-1</sup> )	0.06	0.04	0.80	0.05	1.17	0.55	0.43
<b>RSD (%)</b>	<b>0.54</b>	<b>1.34</b>	<b>0.59</b>	<b>0.50</b>	<b>1.68</b>	<b>0.92</b>	<b>1.07</b>

Table 2

Date	Number of measurements	RSD (%)						
		Mg <sup>2+</sup>	K <sup>+</sup>	Ca <sup>2+</sup>	Na <sup>+</sup>	SO <sub>4</sub> <sup>2-</sup>	NO <sub>3</sub> <sup>-</sup>	Cl <sup>-</sup>
20 <sup>th</sup> July 2015	(22)	0.17	0.90	0.21	0.22	0.39	0.47	0.24
28 <sup>th</sup> August 2015	(20)	0.32	0.63	0.31	0.36	0.20	0.25	0.19
17 <sup>th</sup> April 2016	(35)	0.38	1.20	0.17	0.31	0.31	0.38	0.30